AD-A032 047 NAVAL RESEARCH LAB WASHINGTON D C F/G 20/5
A DYNAMICAL MODEL FOR MAGNETIC SIGNAL INTERPRETATION IN RELATIV--ETC(U)
OCT 76 K R CHU, R W CLARK

UNCLASSIFIED NRL-MR-3386 NL

1 OF 1
ADA032047

END
DATE
FILMED
1 -77

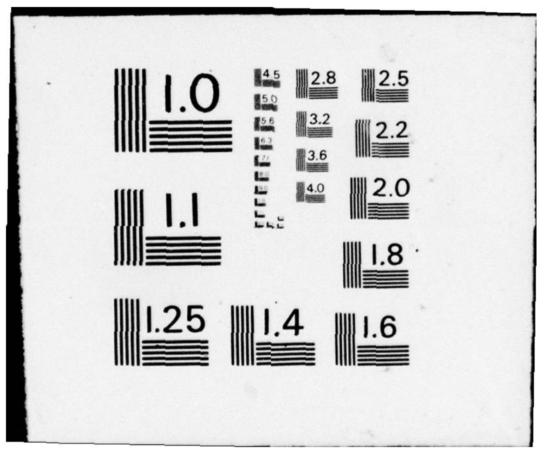
1.0
1.1
1.25
1.4
1.6
1.8
2.0
2.2
2.5
2.8
3.2
3.6
4.0
4.5
5.0
5.6
6.3

(12)

NRL Memorandum Report 3386

A Dynamical Model for Magnetic Signal Interpretation in Relativistic Electron Beam Heated Plasmas

K. R. Chu

Science Applications, Inc.
McLean, Virginia

and

R. W. Clark

Plasma Dynamics Branch
Plasma Physics Division

October 1976

NAVAL RESEARCH LABORATORY
Washington, D.C.

SECURITY CLASSIFICATION OF THIS PAGE (When Data Entered)

REPORT DOCUMENTATION PAGE		READ INSTRUCTIONS BEFORE COMPLETING FORM
1. REPORT NUMBER NRL Memorandum Report 3386	2. GOVT ACCESSION NO.	3. RECIPIENT'S CATALOG NUMBER
4. TITLE (and Subtitle) A DYNAMICAL MODEL FOR MAGNETIC SIGNAL INTERPRETATION IN RELATIVISTIC ELECTRON BEAM HEATED PLASMAS		5. TYPE OF REPORT & PERIOD COVERED Interim report on a continuing NRL problem. 6. PERFORMING ORG. REPORT NUMBER
7. AUTHOR(s) K.R. Chu* and R.W. Clark		8. CONTRACT OR GRANT NUMBER(s)
9. PERFORMING ORGANIZATION NAME AND ADDRESS Naval Research Laboratory Washington, D.C. 20375		10. PROGRAM ELEMENT, PROJECT, TASK AREA & WORK UNIT NUMBERS NRL Problem H02-28B
11. CONTROLLING OFFICE NAME AND ADDRESS Office of Naval Research Arlington, Virginia 22217		12. REPORT DATE October 1976 13. NUMBER OF PAGES 22
14. MONITORING AGENCY NAME & ADDRESS(if different from Controlling Office) 12 13p.		15. SECURITY CLASS. (of this report) UNCLASSIFIED 15a. DECLASSIFICATION/DOWNGRADING SCHEDULE

9 | 6 | 10 | 11 | 14 NRL-MR-3386

16. DISTRIBUTION STATEMENT (of this Report)

Approved for public release; distribution unlimited.

17. DISTRIBUTION STATEMENT (of the abstract entered in Block 20, if different from Report)

18. SUPPLEMENTARY NOTES

This work was supported by the Office of Naval Research.

*Present address: Science Applications, Incorporated, 8400 Westpark Drive, McLean, Virginia 22101.

19. KEY WORDS (Continue on reverse side if necessary and identify by block number)

Electron beam
Heating
Magnetic probe

20. ABSTRACT (Continue on reverse side if necessary and identify by block number)

A dynamical model is developed to infer the plasma energy from local and global magnetic field measurements. Physical processes involved are macroscopic and observable. Scaling laws provide further checks. This model, when applicable, should be employed to estimate the plasma energy in rapidly pulsed heating experiments, where static pressure balance models have been commonly used.

DD FORM 1 JAN 73 1473 EDITION OF 1 NOV 65 IS OBSOLETE
S/N 0102-014-6601

SECURITY CLASSIFICATION OF THIS PAGE (When Data Entered)

251 950 LB

SECURITY CLASSIFICATION OF THIS PAGE(When Data Entered)

A DYNAMICAL MODEL FOR MAGNETIC SIGNAL INTERPRETATION IN RELATIVISTIC ELECTRON BEAM HEATED PLASMAS

In recent years, many experimental efforts[1-11] have been made to achieve rapid plasma heating by the use of intense relativistic electron beams. Typically, a beam of 50-200 nsec duration is injected into a plasma or neutral gas column magnetized by a uniform magnetic field B_0. In such experiments, the most commonly used diagnostic tool to measure the plasma energy is either a magnetic probe or a diamagnetic loop. To calculate the plasma perpendicular energy density $W_\perp$ from the probe or loop measurements, a sharp boundary static pressure balance model is commonly assumed. For example, if δB_z is the measured (para) magnetic field variation between the hot plasma and a metallic wall of radius r_w then from the pressure balance equation,

$$B_{zi}^2 + 8\pi W_\perp = (B_0 + \delta B_z)^2 \tag{1}$$

where B_{zi} is the magnetic field inside the hot plasma, and invoking conservation of magnetic flux, $W_\perp$ can be expressed as

$$W_\perp \simeq \frac{1}{4\pi} \left(\frac{r_w}{r_{eq}}\right)^2 B_0 \, \delta B_z, \text{ for } \delta B_z << B_0 \tag{2}$$

where r_{eq} is the hot plasma radius at equilibrium.

However, static models are not always valid. Under some conditions (discussed below), the establishment of a plasma equilibrium after rapid beam energy deposition involves relatively slow mass motion of the plasma; consequently, on the time scale of the experiment, the equilibrium state indicated by Equation 1 cannot be reached.

Furthermore, the measured δB_z under such conditions may be the amplitude of a magnetosonic wave, instead of the depth of a magnetic well. Therefore, an alternative model is needed when the validity of the static model becomes questionable.

Note: Manuscript submitted September 20, 1976.

Physically, two limiting regimes can be distinguished--the resistive[12,13] regime and the reactive[16] regime. If

$$\tau_i \text{ and/or } \tau_m << \tau_A \tag{3}$$

where τ_i is the ion collision time, τ_m is the magnetic diffusion time, and $\tau_A \equiv r_b/v_A$ (r_b is the beam radius, v_A is the Alfven speed), the system is in the resistive regime and is characterized by magnetic diffusion processes[12-15]. The correlation between (the nonoscillatory) δB_z and a given diamagnetic current in this regime has been discussed by Guillory and Bailey[14], and Striffler and Kapetanakos[15]. In the reactive regime,

$$\tau_i \text{ and } \tau_m << \tau_A \tag{4}$$

the system is characterized by gross plasma motions, namely, magnetosonic oscillations[16, 17]. The latter regime applies to plasmas with sufficiently high temperatures. Recently, oscillatory magnetic signals have been reported[5,7,9,10] and identified[5,7,9] as magnetosonic oscillations. With improved heating, future experiments are likely to be in this regime also. Hereafter, we will be concerned with this regime only.

It is important to distinguish two cases according to experimental conditions. Case 1: the hot plasma is surrounded by vacuum or by a neutral gas; Case 2: it is surrounded by a cold plasma. For case 1, B_z between the plasma and the wall, though oscillatory, is spatially uniform (Fig. 1a), thus the static model gives a reasonable estimate of $W_\perp$ provided one takes the time averaged δB_z and determines r_{eq} consistently. For case 2, on the other hand, the probe or loop (immersed in the cold plasma) will measure a magnetosonic wave (Fig. 1b) generated by the beam energy deposition and the correlation between δB_z and $W_\perp$ is determined by the dynamics of the plasma, rather than by the condition of static pressure balance. The implication of δB_z in this case is thus qualitatively different from that of case 1. For example, roughly speaking, the wall would have no effect on the peak probe signal if $r_o \lesssim \frac{4}{5} r_p$ and it has no effect on the peak loop signal if $r_o \lesssim \frac{2}{3} r_p$, where r_p is the plasma radius, r_o is the probe position for loop radius and we have assumed constant wave speed. Clearly, if the above conditions are satisfied, $W_\perp$ given by Eq. (2), which scales as r_w^2, is inapplicable.

In most experiments,[1-6,9,11] the plasma is preformed by a discharge; it is reasonable that in these experiments case 2 prevails. To the authors' knowledge, a proper theoretical model to interpret probe or loop data for case 2 in the reactive regime has hitherto been lacking, although there are ample experimental evidences that this regime has indeed been observed. In the following, we develop a dynamical model applicable to this regime.

Formulation

We make the following assumptions: (1) $\partial/\partial\Theta = \partial/\partial z = 0$; (2) $v_{iz} = v_{ez} = 0$; (3) initially uniform plasma ($n=n_o$) maintaining quasineutrality; this, together with the previous two assumptions, implies $v_{er} = v_{ir} = v_r$; (4) $v_A \ll c$; (5) neglecting electron inertia and ion pressure; (6) neglect electron and ion collisions; (7) neglect radial thermal conduction--this requires $(r_b/\rho_e)^2 \nu_e^{-1} \gg \tau_A$, where ρ_e is the electron Larmor radius and ν_e is the electron collision frequency; (8) neglect wall effect; and (9) isotropic electron velocity distribution. The system is then described by

$$\left(\frac{\partial}{\partial \bar{t}} + \bar{v}_r \frac{\partial}{\partial \bar{r}}\right)\bar{v}_r = \bar{E}_r \tag{5}$$

$$\bar{B}_z \frac{\partial}{\partial \bar{r}} \bar{B}_z = -\bar{n}\,\bar{E}_r - \frac{1}{2}\frac{\partial}{\partial \bar{r}} \bar{p}_e \tag{6}$$

$$\overline{B}_z \overline{v}_r = \overline{E}_\Theta \tag{7}$$

$$\frac{1}{\overline{r}} \frac{\partial}{\partial \overline{r}} (\overline{r}\overline{E}_\Theta) = - \frac{\partial}{\partial \overline{t}} \overline{B}_z \tag{8}$$

$$\frac{\partial}{\partial \overline{t}} \overline{n} + \frac{1}{\overline{r}} \frac{\partial}{\partial \overline{r}} (\overline{r}\, \overline{n}\, \overline{v}_r) = 0 \tag{9}$$

$$\left(\frac{\partial}{\partial \overline{t}} + \overline{v}_r \frac{\partial}{\partial \overline{r}}\right)(\overline{p}_e \overline{n}^{-\frac{5}{3}}) = \frac{2}{3} \overline{n}^{-\frac{5}{3}} \overline{Q}_b \tag{10}$$

where overbars represent normalized quantities defined as follows: $\overline{t} \equiv t/\tau_A$, $\overline{r} \equiv r/r_b$, $\overline{n} \equiv n/n_o$, $\overline{p}_e \equiv 8\pi nkT_e/B_o^2$, $\overline{B}_z \equiv B_z/B_o$, $\overline{E}_r \equiv E_r r_b e/m_i v_A^2$, $\overline{E}_\Theta \equiv E_\Theta c/v_A B_o$, $\overline{v}_r \equiv v_r/v_A$, $\overline{Q}_b \equiv Q_b\ 8\pi\tau_A/B_o^2$ and Q_b is the rate of beam energy deposition per unit volume. We let

$$\overline{Q}_b = \begin{cases} \dfrac{\pi(s+2)}{2s\overline{\tau}_b} \beta_E[1-\overline{r}^{-s}] \sin \dfrac{\pi\overline{t}}{\overline{\tau}_b}, & \text{if } \overline{r} \leq 1,\ \overline{t} \leq 1 \\ 0\quad, & \text{otherwise} \end{cases}$$

where $\overline{\tau}_b = \tau_b/\tau_A$ is the normalized beam duration, the free parameter $\beta_E = \frac{1}{\pi}\int_0^1 2\pi\overline{r}d\overline{r} \int_0^{\overline{\tau}_b} d\overline{t}\ \overline{Q}_b$, is the space and time integrated beam energy deposition scaled to the total external magnetic field energy within the beam volume ($r \leq r_b$) and s is a steepness parameter to account for the spatial inhomogeneity of beam energy deposition. Note that the only parameters to specify are those contained in $\overline{Q}_b$ (i.e., s, $\overline{\tau}_b$, and β_E). All other parameters such as B_o, n_o, r_b, etc., are scaled out of Eqs. (5)-(10) through normalization.

Solutions

The radial one-dimensional evolution of the system is computed from Eqs. (5)-(10) using a hydromagnetic code which employs a two-step Lax-Wendroff flux corrected transport (FCT) algorithm.[18,19]

Results of our calculations are schematically presented. Figure 2a shows typical radial profiles of $\overline{B}_z$. Figure 2b plots typical probe signals $[\delta\overline{B}_z(\overline{r}_o)]$ and loop signals

$$\delta\overline{\phi}(\overline{r}_o) \equiv \int_o^{\overline{r}_o} d\overline{r}'\ 2\pi\overline{r}'\ \delta\overline{B}_z(\overline{r}')$$

as would be measured by a probe or loop with $\overline{r}_o = 1.2$. If a conducting wall is present, wave bouncing will predictably produce a second, third peak, and so on.

Figures 3a and b plot the peak probe signals $(\delta\overline{B}_z^p)$ and loop signals $(\delta\overline{\phi}^p)$ versus the total energy deposited (β_E). Each family of curves is generated by the parameter $\overline{\tau}_b$. We note that for the same amount of energy deposited, a faster rate of deposition (i.e., smaller $\overline{\tau}_b$) results in larger wave amplitude (see the $\delta\overline{B}_z^p$ curves), and stronger dispersion or nonlinearity (see the bending of the $\delta\overline{\phi}^p$ curves). Such differences can be distinguished in the present dynamical model, but not in the static model. Since $\delta\overline{B}_z^p$ is a local quantity and $\delta\overline{\phi}^p$ is a global quantity, $\overline{\tau}_b$ has less effect on the latter.

All calculations presented so far are for the steepness parameter s=2. We have varied s in our runs and found that the s=1 case gives slightly (<15%) higher $\delta\overline{B}_z^p$ and the s=3 case gives slightly (<10%) lower $\delta\overline{B}_z^p$. The effect of s on $\delta\overline{\phi}^p$ is much weaker.

Because of the normalized parameter system employed here, the data shown in Figs. 3a and b have general applicability. As an example, consider the Physics International experiment recently reported by Prono, et al.[10] Their high ν/γ beam heating scheme produced an impressive plasma energy density as high as 10^{19} eV/cm^3. There is little question that the experiment was in the reactive regime. The static model that they used to interpret the probe signal is appropriate for the situation depicted in Fig. 1a. If the situation was more like Fig. 1b instead,[21] then the dynamical model should have been used. In any case, it is interesting to compare their interpretations with those given by the dynamical model. Using their published data, we obtain $\overline{r}_o \simeq 1.2$, $\overline{\tau}_b \simeq 1\text{-}2$, and $\delta\overline{B}_z^p \simeq 0.1$, thus from Fig. 4a, $\beta_E \simeq 0.7\text{-}1.0$, which corresponds to an average plasma energy density[20] of $4\text{-}6 \times 10^{18}$ eV/cm^3, in agreement with their interpretations. We point out, however, that the agreement between the two interpretations is coincidental in view of the qualitative differences between the models used.

Finally, if either collisions (magnetic diffusion effect) or thermal conduction (cooling effect) were included in our model, the calculated signals ($\delta\overline{B}_z^p$ and $\delta\overline{\phi}^p$) would be weaker. Thus, β_E inferred from the present model yields a conservative estimate of beam energy deposition.

The authors would like to thank Drs. D. Book, D. A. Hammer, and C. C. Wei for helpful discussions.

REFERENCES

1. A. T. Altyntsev, A. G. Es'kov, O. A. Zolotovskii, V. I. Koroteev, R. Kh. Kurtmullaev, V. D. Masalov, and V. N. Semenov, ZhETF Pis. Red. 13, No. 4, 197 (1971) [Sov. Phys. JEPT Lett. 13, 139 (1971)].

2. D. R. Smith, Phys. Letters A 42, 211 (1972).

3. P. A. Miller, and G. W. Kuswa, Phys. Rev. Letters 30, 958 (1973).

4. C. A. Kapetanakos and D. A. Hammer, Appl. Phys. Letters 23, 17 (1973).

5. Yu. I. Abrashitov, V. S. Koidan, V. V. Konyukhov, V. M. Lagunov, V. N. Luk'yanov, K. I. Mekler and D. D. Ryutov, Zh. Eksp. Teor. Fiz. 66, 1324 (1974) [Sov. Phys. - JETP 39, 647 (1974)].

6. G. C. Goldenbaum, W. F. Dove, K. A. Gerber and B. G. Logan, Phys. Rev. Lett. 32, 830 (1974).

7. C. Ekdahl, M. Greenspan, R. E. Kribel, J. Sethian and C. B. Wharton, Phys. Rev. Lett. 33, 346 (1974).

8. J. P. Vandevender, J. D. Kilkenny and A. E. Dangor, Phys. Rev. Lett. 33, 689 (1974).

9. C. A. Kapetanakos, W. M. Black and K. R. Chu, Phys. Rev. Lett. 34, 1156 (1975).

10. D. Prono, B. Ecker, N. Bergstrom and J. Benford, Phys. Rev. Lett. 35, 438 (1975).

11. W. F. Dove, K. A. Gerber and D. A. Hammer, Appl. Phys. Lett. 28, 173 (1976).

12. K. R. Chu and N. Rostoker, Phys. of Fluids 17, 813 (1974).

13. K. Molvig, N. Rostoker and F. Dothan, Plasma Physics and Controlled Nuclear Fusion Research, Proceedings of the Fifth International Conference, Tokyo (IAEA, Vienna, 1975), Vol. 3, p. 249.

14. J. Guillory and V. Bailey, Bull. Am. Phys. Soc. 18, 1349 (1973).

15. C. D. Striffler and C. A. Kapetanakos, J. Appl. Phys. 46, 2509 (1975).

16. K. R. Chu, C. A. Kapetanakos and R. W. Clark, Appl. Phys. Lett. 27, 185 (1975).

17. K. R. Chu, R. W. Clark, M. Lampe, P. C. Liewer and W. M. Manheimer, Phys. Rev. Lett. 35, 94 (1975).

18. J. P. Boris and D. L. Book, J. Comp. Phys. 11, 38 (1973).

19. D. L. Book, J. P. Boris and K. Hain, J. Comp. Phys. 18, 248 (1975).

20. The present fluid model only gives isotropic energy density. It cannot distinguish the Maxwellian distribution from, for example, the two-bump distribution.

21. Experimentally, this question can be resolved by measuring $\delta\bar{B}_z$ at two radial positions outside the beam channel and observing their phase relationship.

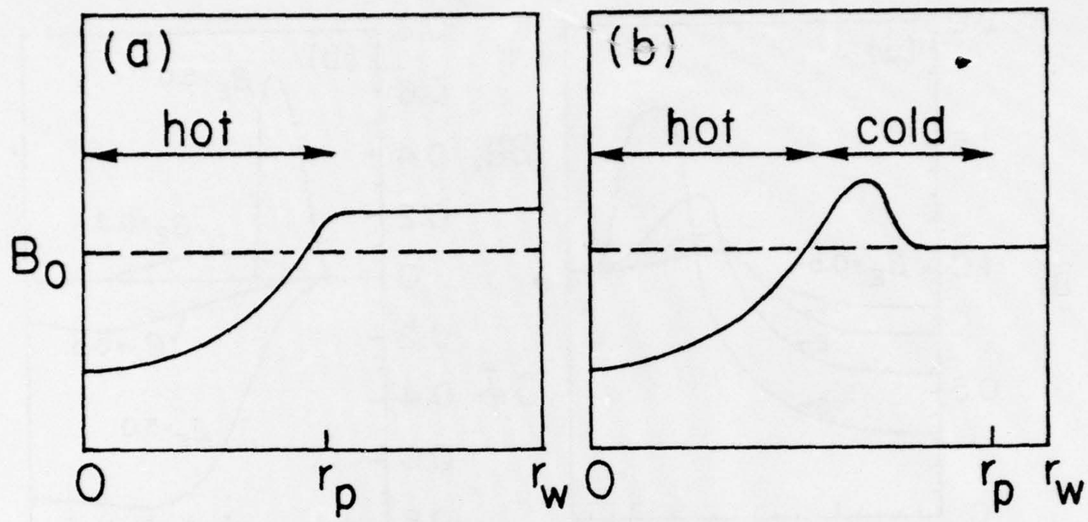

Fig. 1 — Qualitative profile of B_z after beam energy deposition; (a) hot plasma surrounded by vacuum or neutral gas, (b) hot plasma surrounded by cold plasma

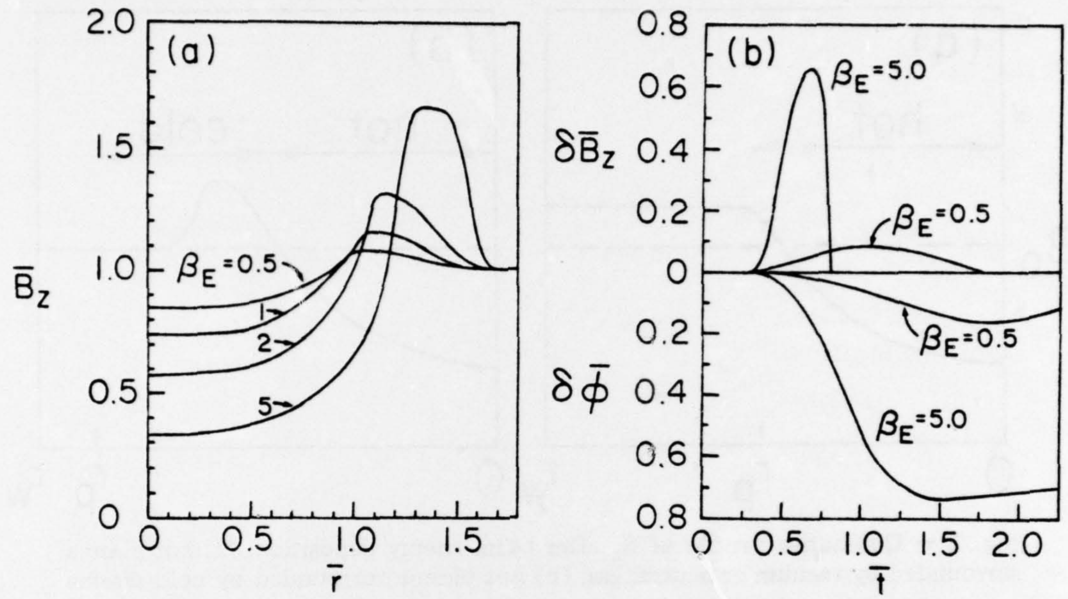

Fig. 2 — (a) Typical radial profiles of $\overline{B}_z$ at $\overline{t}$ = 0.75 as computed from Eqs. (5)-(10). (b) Typical probe signals ($\delta\overline{B}_z$) and loop signals ($\delta\overline{\phi}$) at probe position (or loop radius) $\overline{r}_o$ = 1.2. For both figures, s = 2, $\overline{\tau}_b$ = 0.5.

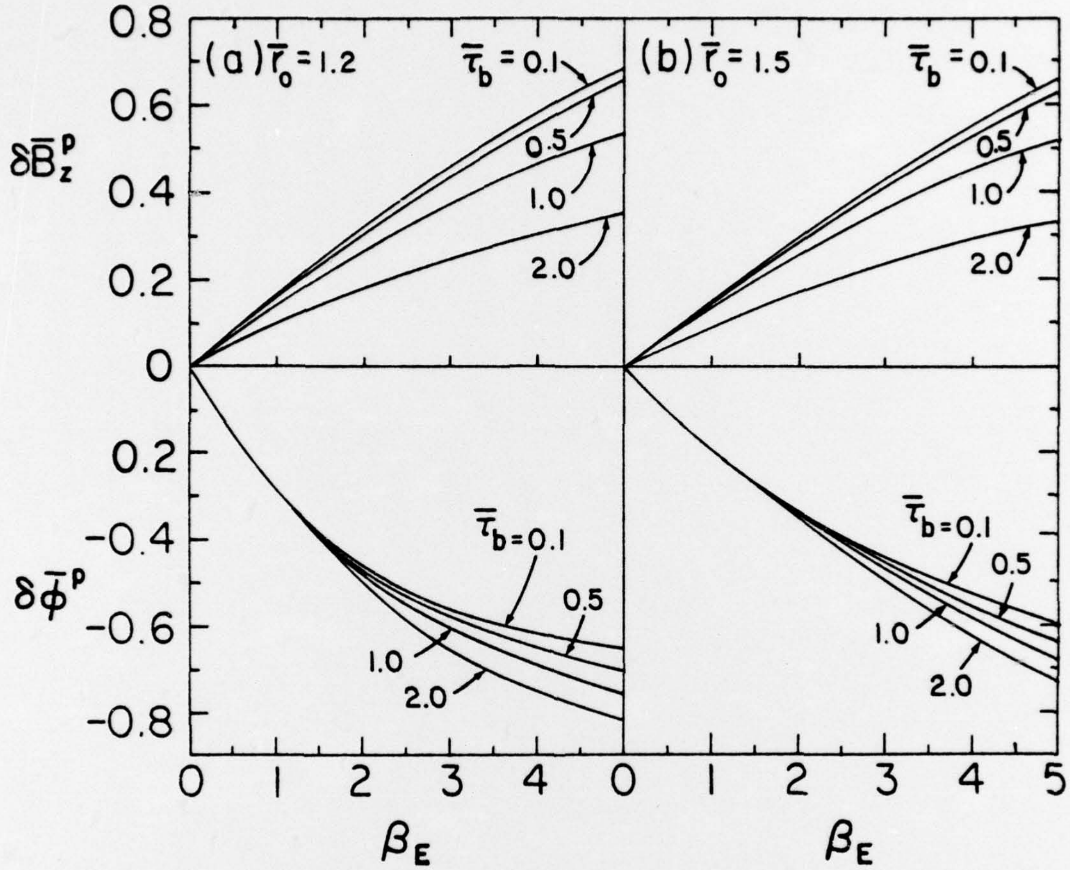

Fig. 3 — Peak probe signals ($\delta\bar{B}_z^p$) and peak loop signals ($\delta\bar{\phi}^p$) versus β_E, for s = 2

DISTRIBUTION LIST

DIRECTOR
Naval Research Laboratory
Washington, D.C. 20375
ATTN: HDQ COMM DIR Bruce Wald

DIRECTOR
Naval Research Laboratory
Washington D. C. 20375
ATTN: CODE 5460 Radio Propagation BR

DIRECTOR
Naval Research Laboratory
Washington, D. C. 20375
ATTN: CODE 7127, Charles Y. Johnson

DIRECTOR
Naval Research Laboratory
Washington, D. C. 20375
ATTN: CODE 7701 Jack D. Brown

DIRECTOR
Naval Research Laboratory — 25 copies
Washington, D. C. 20375
ATTN: CODE 7700, Division Superintendent

DIRECTOR
Naval Research Laboratory — 150 copies
Washington, D.C. 20375
ATTN: CODE 7750, Branch Head

COMMANDER
Naval Space Surveillance System
Dahlgren, Va. 22448
ATTN; CAPT. J. H. Burton

COMMANDER
Naval Surface Weapons Center
White Oak, Silver Spring, Md. 20910
ATTN; CODE 730 Tech. Lib.

COMMANDER
Naval Surface Weapons Center
White Oak, Silver Spring, Md. 20910
ATTN; CODE 1224 Navy Nuc Prgms Office

DIRECTOR
Strategic Systems Project Office
Navy Department
Washington, D. C. 20376
ATTN: NSP-2141

COMMANDER
ADC/AD
ENT AFB CO 80912
ATTN: ADDA

AF Cambridge Rsch Labs, AFSC
L. G. Hanscom Field
Bedford, MA 01730
ATTN: LKB Kenneth S. W. Champion

AF Cambridge Rsch Labs, AFSC
L. G. Hanscom Field
Bedford, MA 01730
ATTN: OPR Hervey P. Gauvin

AF Cambridge Rsch Labs, AFSC
L. G. Hanscom Field
Bedford, MA 01730
ATTN: OPR James C. Ulwick

AF Weapons Laboratory, AFSC
Kirtland AFB, NM 87117
ATTN: DYT LT Mark A. Fry

AF Weapons Laboratory, AFSC
Kirtland AFB, NM 87117
ATTN: DYT CAPT Whittwer

AF Weapons Laboratory, AFSC
Kirtland AFB, NM 87117
ATTN: John M. Kamm SAS

AF Weapons Laboratory, AFSC
Kirtland AFB, NM 87117
ATTN: SUL

AFTAC
Patrick AFB, FL 32925
ATTN: TF MAJ. E. Hines

AFTAC
Patrick AFB, FL 32925
ATTN: TF/CAPT. Wiley

Massachusetts Institute of Technology
Lincoln Laboratory
244 Wood Street
Lexington, Mass. 02173
ATTN: J. Evans and D. Towle

University of Pittsburgh of the Commonwealth
System of Higher Education
Cathedral of Learning
Pittsburgh, Pa. 15213
ATTN: C. Ray, Security Officer
Prof. Wade Fite
Dr. F. Kaufman, 205 SRCC Bldg.

AVCO-EVERETT Research Laboratory
2585 Revere Beach Parkway
Everett, Mass. 02149
Attn: Technical Library
Attn: Dr. R. Patrick and Dr. J. Workman

Bell Telephone Labs., Inc.
Whippany Road
Whippany, New Jersey 07981
ATTN: Lyman Fretwell

General Electric Company
Tempo-Center for Advanced Studies
816 State Street
Santa Barbara, California 93102
ATTN: W. Chan, Robert L. Bogusch,
Warren Knapp, DNA Information
and Analysis Center

General Research Corporation
P.O. Box 3587
Santa Barbara, Calif. 93105
ATTN: Dr. John Ise

Director
Defense Research and Engineering
Washington, D. C.
ATTN: Deputy Dir. Res. and Advanced Tech.

Director
Advanced Research Projects Agency
Washington, D. C. 20301
ATTN: LtC Wm. Whitaker

Director
Defense Nuclear Agency
6801 Telegraph Road
Alexandria, Va. 20305
ATTN: RAAE
ATTN: Technical Library (STTL)
ATTN: RAEV
ATTN: STUL

Commander
Field Command
Defense Nuclear Agency
Albuquerque, New Mexico 87115

Director
Defense Intelligence Agency
Washington, D.C. 20301
ATTN: Reference Library Branch

Commander
Harry Diamond Laboratories
2800 Powder Mill Road
Adelphia, Md. 20783
ATTN: DRXDC-TD

Director
Ballistic Missile Defense Advanced Technical Center
Huntsville Office
P.O. Box 1500
Huntsville, Alabama 35807
ATTN: Melvin T. Capps
ATC-T

Director
Ballistic Missile Defense Program Officer
Commonwealth Bldg.,
Arlington, Va. 22209
ATTN: Dep BMDPM Mr. Julian Davidson
Mr. Archie Gold

Director
US Army Ballistic Research Laboratories
Aberdeen, Maryland
ATTN: Mr. Frank Niles

Dr. J. Martineau
Centre de l'Energie
University of Quebec, INRS CP 1020
Varennes, Quebec, CANADA

Dr. R. Papoular
Comm. Energie Atomique - France
B. P. No. 6 - Fontenay - Aux - Roses - 92
France

Dr. Ralph Rudder
Air Force Weapons Laboratory
LRE - Kirkland AFB
New Mexico 87117

Dr. David Smith
United Aircraft Research Laboratories
400 East Main Street
East Hartford, Conn. 06108

Dr. R. G. Tomlinson
United Aircraft Research Laboratories
Silver Lane
E. Hartford, Conn. 06108

Dr. Robert Turner
Applied Physics Laboratory
Johns Hopkins
8621 Georgia Avenue
Silver Spring, Md. 20910

Dr. George Vlaska
Aerospace Research Laboratory
University of Washington
Seattle, Washington 98105

Dr. H. J. Kunze
Abteilung fur Physik und Astronomie, Ruhr - Universitat
463 Bochum
Postfach 2148
West Germany

Dr. A. W. DeSilva/Dr. R. C. Davidson/ Dr. J.U. Guillory
University of Maryland
Department of Physics and Astronomy
College Park, Maryland 20742

Dr. A. J. Alcock
National Research Council
Physics Division
100 Sussex Drive
Ottawa, Ontario, Canada

Dr. Martin C. Richardson
National Research Council
Physics Division
100 Sussex Drive
Ottawa 2, Ontario, CANADA

Dr. Keith Boyer
Los Alamos Scientific Laboratory
P.O. Box 1663
Los Alamos, New Mexico 87544

Dr. John W. Deiber
Dr. Ron Rehm
Cornell Aeronautical Laboratory
4455 Genesee Street
Buffalo, New York 14221

Dr. D. F. Dubois
Hughes Research Laboratories
3011 Malibu Canyon Road
Malibu, California 90265

Dr. A. G. Engelhardt
Hydro-Quebec Institute of Research
1800 Montee Ste-Julie, Varennes
P. Q., Canada

Dr. T. V. George
Westinghouse Research Labs. Pgh.
Pittsburgh, Pa. 15235

Dr. Martin V. Goldman
Department of Astro-Geophysics
University of Colorado
Boulder, Colorado 80302

Dr. Arthur H. Guenther
Air Force Weapons Laboratory (S.Y.)
Kirtland Air Force Base
Albuquerque, New Mexico 87117

Mr. Roger Case
Air Force Weapons Laboratory
Kirtland Air Force Base
Albuquerque, New Mexico 87117

Dr. Eric D. Jones
Sandia Laboratories
Div. 5214
P.O. Box 5800
Albuquerque, New Mexico 87115

Dr. Moshe J. Lubin
University of Rochester
Laboratory for Laser Energeties
Mech. and Aerospace Sciences, Dept.
Rochester, N. Y. 14627

Dr. Philip Mallozzi
Battelle Memorial Institute
Dept. of Physics
505 King Avenue
Columbus, Ohio 43201

Dr. James Shearer
Lawrence Livermore Lab.
P. O. Box 808
Livermore, California 94551

Dr. Donald W. Kerst/ Dr. R. S. Post
University of Wisconsin
Sterling Hall
Department of Physics
Madison, Wisconsin 53706

Prof. J. G. Hirschberg, Jr.
University of Miami
Department of Physics
Coral Gables, Florida 33124

Dr. L. P. Bradley
Lawrence Livermore Laboratory
P.O. Box 808
Livermore, Calif. 94551

Prof. Frank Chen / Prof. M.C. Luhmann
Department of Engineering
University of California
Los Angeles, Calif. 90024

Prof. Alfred Wong / Prof. J. Dawson
Department of Physics
University of California
Los Angeles, Calif. 90024

Dr. Stephen O. Dean
Division of Research
Energy Research and Development Administration
Washington, D.C. 20545

Dr. Roy Gould
Cal. Inst. Tech.
Pasadena, Calif. 91109

Dr. J. Decker/ Dr. W. F. Dove
DCTR
Energy Research and Development Administration
Washington, D. C. 20545

Mr. W. C. Gough / F. R. Scott
Electric Power Research Institute
Washington, D.C. 20545

Dr. S. J. Buchsbaum
Bell Telephone Labs
P. O. Box 262
Murray Hill, N. J. 07904

Dr. D. J. Rose
Oak Ridge National Lab.
P. O. Box X
Oak Ridge, Tenn. 37830

Dr. A. E. Ruark
7952 Orchid St. N. W.
Washington, D.C. 20012

Maxwell Laboratories
9244 Balboa Avenue
San Diego, California 92123
ATTN: Dr. A. C. Kolb
Dr. Peter Korn
Dr. V. Fargo
Mr. J. Shannon

Dr. A. F. Haught
39 Fox Den Road
Glastonburg, Conn. 06033

Dr. F. J. Fader
197 Foote Road, S.
Glastonburg, Conn. 06073

Dr. Fred Schwirzke
Naval Postgraduate School
Monterey, Calif. 92940

Dr. M. B. Gottlieb
Forrestal Research Center
P. O. Box 451
Princeton, N. J. 08540

Dr. F. L. Ribe
P. O. Box 1663
Los Alamos, New Mexico 87544

Dr. T. K. Fowler
Lawrence Livermore Lab.
P. O. Box 808
Livermore, Calif. 94551

Dr. Herman Postma
Bldg. 9201-2 336
T-12
Oak Ridge, Tenn. 73830

Dr. J. Rand McNally
103 Norman Lane
Oak Ridge, Tenn. 73830

Dr. Wulf Kunkel
Dept. of Physics
University of California
Berkeley, Calif. 94720

Dr. Harry Dreicer
P.O. Box 1653
Los Alamos, New Mexico 87544

Dr. Franz Johoda
P. O. Box 1663
Los Alamos, New Mexico 87544

Dr. Ralph Lovberg
4744 Panorama Drive
San Diego, Calif. 92116

Dr. Herbert W. Friedman
Avco Everett Res. Labs.
2585 Revere Beach Parkway
Everett, Mass. 02149

Cornell University
Ithaca, New York 14850
ATTN: Dr. David Morse
Dr. R. N. Sudan
Dr. C. B. Wharton
Dr. Hans Fleischman
Dr. J. A. Nation

Dr. Joseph Fergusen
Dept. of Physics
Mississippi State University
State College, Miss. 39762

Dr. Robert J. Mackin, Jr.
2622 N. Holliston
Altadena, Calif. 91001

Dr. David R. Bach
8 Heatheridge
Ann Arbor, Mich. 48104

Dr. Richard Hall
1851 111 E. N. E.
Bellevue, Washington 98004

Dr. Lawrence Lidsky
1784 Washington St.
Newton, Mass. 02166

H. Ahlstrom / L. Steinberg
Dept. of Aeronautics and Astronautics
Univ. of Washington
Seattle, Wash. 98105

Dr. David Koopman
Inst. Fluid Dynamics
University of Maryland
College Park, Md. 20740

Columbia University
New York, N. Y. 10023
ATTN: Dr. Robert Gross
Dr. S. P. Schlesinger